URSI GASS 2020, Rome, Italy, 29 August - 5 September 2020

A multi-stage pass-band filter with ultra-compact spiral-based elements

Alessandro Cidronali, Giovanni Collodi, Matteo Lucchesi, Stefano Maddio, Giuseppe Pelosi, Stefano Selleri*
Department of Information Engineering
University of Florence, Via di Santa Marta, 3, Florence, Italy
(alessandro.cidronali,giovanni.collodi,stefano.maddio,giuseppe.pelosi,stefano.selleri)@unifi.it
matteo.lucchesi4@stud.unifi.it

Abstract

Recently an innovative pass-band filter based on a disk with a pair of spiral slot etched has been presented in literature. Such a filter has an out-of-band steep descent of the transmission coefficient but a relatively poor insertion loss for frequencies far from the pass-band. In this contribution a multi-stage set up of these filters is proposed to ameliorate the rejected bands insertion loss. The proposed filter is still extremely compact if compared to filters with similar behavior.

1 Introduction

C-band is extensively used for many applications: 802.11xy WiFi from 4.9 to 5.7 GHz, DSRC at 5.8 GHz, WAVE protocol at 5.9 GHz, Mid-Band 5G, just to name few. Yet, the sheer number of services provided on different protocols exploiting narrowly separated bands can cause severe interference problems, especially in vehicular applications [1, 2]. Several solutions are possible, ranging from active ones, such as leakage cancellers [3, 4, 5] to passive ones, such as electronic band-gap [6, 7], or even sharp roll-off filters [8, 9, 10].

Recently a compact and uniplanar structure based on a disc resonator in microstrip technology has been presented [11]. The design of the cited filter is reported in Fig. 1. A pair of antipodal Archimedean spirals are etched inside the disc which is obtained enalarging a transmission lines of length w. The structure equivalent circuit [11], depicted in Fig. 1 as well, shows a quasi-elliptical response with sharp nulls outside the pass-band, similar to [12]. The Archimedean spiral is defined according to:

$$p(\theta) = (R-g)(1-\alpha\theta), \text{ with } \theta \in [\theta_1, \theta_2], \qquad (1)$$

where R is the radius of the disc, g is the gap between the spiral and the disc edge, α is a factor that controls the distance between successive turns, θ_1 is the starting angle of the spiral, and θ_2 is the end angle, comprehensive of n possible spiral turns.

Notwithstanding a set of parametric analysis reported in [11], which allows for tuning the band and the zeros, the filter presents an insufficient insertion loss in the rejected bands, and let the DC pass. This latter feature might indeed be valuable since DC feed of amplifier can be let through the filter, while rejection is usually important in neighboring bands which may host possibly interfering signals. The key of this paper is hence to produce two tunable stop-bands around the pass-band.

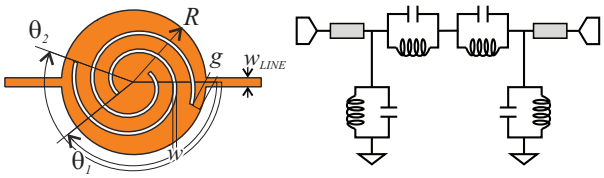

Figure 1. Filtering element layout and equivalent RLC circuit representation.

2 Filter Design

In this contribution a multistage arrangement of these filters is proposed to mitigate the low rejection in the bands neighboring the pass-band without impairing DC. Despite the final structure is an improper band-pass, it is nevertheless very effective for the coexistence of the many services which populate the C-band.

The issue stated in the introduction is best illustrated by Fig. 2b, where the filter proposed in [11] is compared to a filter with similar sharp nulls in literature [13]. Yet the size comparison in Fig. 2b clearly show drastic reduction in size of the spiral filter, whose area is less than $1/25$ with respect to [13].

The basic idea is that the cascading arrangement of two, or more, spiral filters, of different band-width allows to synthesize the desired position for the zeros and enhance to out-of band rejection of the resulting structure. Of course, due to the very small dimensions of the single filter, cascading a few of them still lead to a much more compact layout than that proposed in [13]. Here, the solution based

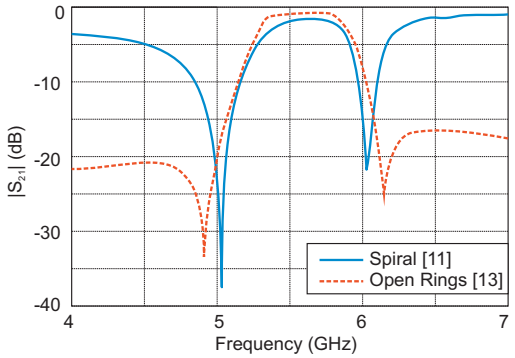

(a) Filter response

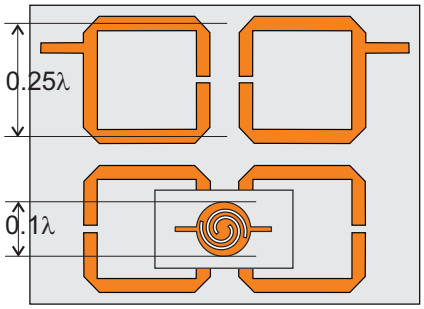

(b) Filter layout

Figure 2. Comparison between the filter element proposed in [11] and the one proposed in [13] (top) and corresponding space occupation comparison (images are in scale) (bottom).

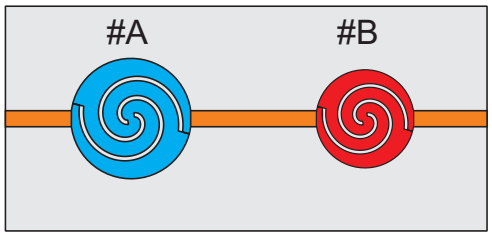

Figure 3. Layout of the cascading of two spiral elements.

on two elements are considered, corresponding to the lay-out depicted in Fig. 3.

Exploiting the peculiar shape of the spiral filter response, two possible solutions for the design of a pass-band device are possible.

With reference to Fig. 4a, in the first case, two spiral elements with similar performance but with different center-frequencies are taken into consideration. They are labeled as #*A* and #*B*. The bandwidth of the two elements are conveniently overlapped, hence the resultant structure exhibit a much marked band-pass behavior. Indeed the transmission is possible only in the frequency range where both #A and #B exhibit low transmission loss. At the same time the resultant structure conserves the transmission zeros of both the element, enforcing the stop-band isolation.

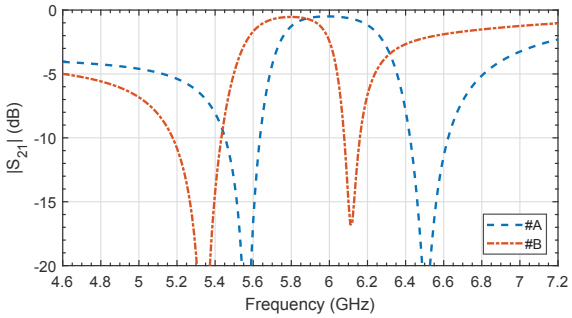

(a) Combination of filters with different bandwidth

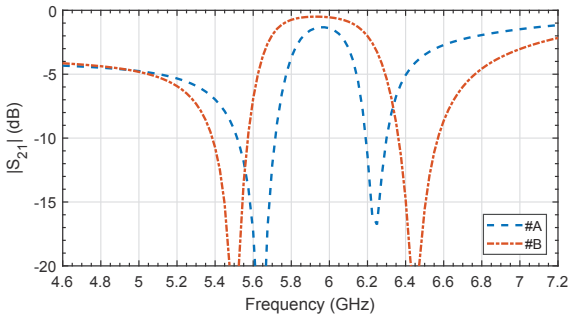

(b) Combination of filters with different center frequencies

Figure 4. Response of two different approaches for the cascading of the filter elements.

In the second case, depicted in Fig. 4b, the two elements are centered on the same reference frequency, but present different bandwidths. In this way, the narrower filter dictated the pass-band of the resulting structure, while the broadband filter imposes a second set of transmission zeroes in addition to the first one, resulting in a frequency behavior similar to that of the previous case.

For the goal of the paper, the second solution has been chosen. The proper disposition of two spiral filters has been arranged on a small printed board, as depicted in Fig. 5a. As explained in [11], the input line suitable for the best performance for the filters is narrow, hence additional line sections for the matching to the system impedance are provided.

A final optimization has been carried. The goals of the optimization are the lowest insertion loss at the center frequency of 5.8 GHz, the highest isolation at 5.3 GHz and 6.3 GHz, as well as the smallest dimension of the resulting design. Due to the multi-objective nature of the goals, the algorithm presented in [14, 15] has been employed.

3 Experimental Validation

With reference to Fig. 5 the design showing the best performance in simulation has been fabricated on commercial dielectric substrate ($\varepsilon_r = 10.0$, $\tan\delta = 0.01$, thickness = 1.27 mm), and experimentally validated. Figure 5b shows a photo of the prototype with the components alongside the lay-out. The calculated final values of the filter parameters

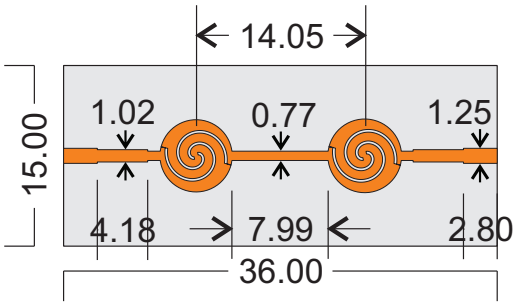

(a) Layout of the pass-band filter

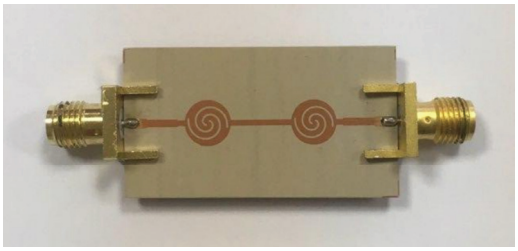

(b) Photograph of the final prototype

Figure 5. Comparison

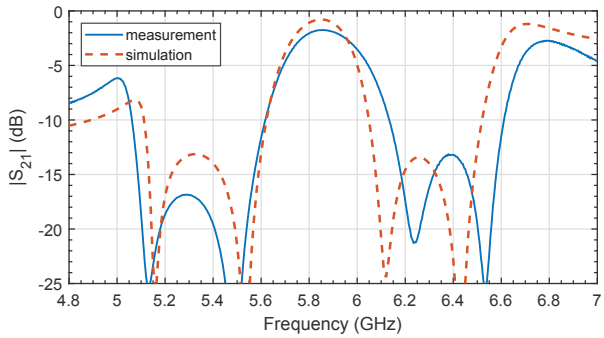

Figure 6. Comparison between the simulated and measured transmission parameters of the proposed filter.

are reported in Table 1. Additional information on the layout are quoted on Fig. 5a.

Finally, Fig. 6 shows the comparison between the simulations and the measurements of the proposed device. Despite a higher loss for the measured filter, probably due to the connectors, the shape of the response is quite matched. A small shift in the upper stop-band is observed, probably due to fabrication tolerance. Indeed, the two pairs of transmission zeroes within the two side stopbands are nevertheless present.

Furthermore, the signal rejection within the two stopbands is higher for the measurement in comparison to the simulations.

4 Conclusions

A multi-stage filter based on extremely compact design is proposed. The proposed device exhibits a local pass-band behavior for application in the C-band. Despite the fact that the actual pass-band behavior is limited in the C-band, the proposed filter is still competitive, being extremely compact if compared to filters with similar behavior.

Table 1. Parameters of the antenna element. All dimensions are expressed in mm, all angles in degrees.

R_A	w_A	g_A	α_A	θ_{A1}	θ_{A2}
3.06	0.23	0.436	0.82	118	195

R_B	w_B	g_B	α_B	θ_{B1}	θ_{B2}
3.00	0.22	0.458	0.77	130	195

The resultant device occupies an area of 3.0×4.5 cm^2, meaning $0.525\lambda_0^2$ at the central frequency of 5.85 GHz. The experimental validations confirm that the performance of the proposed filter, with an insertion loss of -1.8 at center frequency as well as a rejection of about -18.

References

[1] A. Cidronali, S. Maddio, M. Passafiume, G. Manes, "Car talk: technologies for vehicle-to-roadside communications," *IEEE Microw Mag.* **17**, 11, 2016, pp. 40-60.

[2] G. Naik, J. Liu, J.M.J.Park, "Coexistence of dedicated short range communications (DSRC) and Wi-Fi: Implications to Wi-Fi performance," *INFOCOM 2017-IEEE Conference on Computer Communications*, 2017, pp. 1-9.

[3] F. You, G. Chen, "Self-interference cancellations for full-duplex RF front-end using a broadband phase-slope adjuster," *Microw Opt Technol Lett.*, **60**, 6, 2018, pp. 1519-1522.

[4] X. Huang, Y.J. Guo, "Radio frequency self-interference cancellation with analog least mean-square loop," *IEEE Trans. Microw. Theory Tech.*, **65**, 9, 2017, pp. 3336-3350.

[5] S. Maddio, A. Cidronali, G. Manes, "Real-time adaptive transmitter leakage cancelling in 5.8-GHz full-duplex transceivers," *IEEE Trans. Microw. Theory Tech.* **63**, 2, 2015, pp. 509-519.

[6] D. Perez, I. Gil, J. Gago et al. "Reduction of electromagnetic interference susceptibility in small-signal analog circuits using complementary split-ring resonators," *IEEE Trans. Compon. Packag. Manuf. Technol.* **2**, 2, 2012, pp. 240-247.

[7] S. Maddio, G. Pelosi, M. Righini, S. Selleri, I. Vecchi, "Mutual coupling reduction in multilayer patch antennas via meander line parasites," *Electron. Lett.*, **54**, 14, 2018, pp. 922-924.

[8] J.-S.G. Hong, M.J. Lancaster, *Microstrip Filters for RF/Microwave Applications,* New York, NY, John Wiley & Sons, 2004.

[9] R. Gómez-García, A.C. Guyette, D. Psychogiou, E.J. Naglich, D. Peroulis, "Quasi-elliptic multi-band filters with center-frequency and bandwidth tunability," *IEEE Microw Wirel Compon Lett.* **26**, 3, 2016, pp. 192-194.

[10] J. Luo, C. Liao, H. Zhou, X. Xiong, "A novel miniature dual-band bandpass filter based on the first and second resonances for 2.4/5.2 GHz WLAN application," *Microw. Opt. Technol. Lett.*, **57**, 5, 2015, pp. 1143-1146.

[11] A. Cidronali, G. Collodi, S. Maddio, G. Pelosi, S. Selleri, "Quasi-elliptical band-pass filters based on compact spiral resonators for C-band applications," *Microw. Opt. Technol. Lett.*, **61**, 2019, pp. 1983-1987.

[12] K.S.K. Yeo, P. Vijaykumar, "Quasi-elliptic microstrip bandstop filter using tap coupled open-loop resonators," *Prog. Electromagn. Res.*, **35**, 2013, pp. 1-11.

[13] J. Shivhare and B. Reddy, "Design and development of a single fold hairpin line microstrip bandpass filter at 3250 mhz for s-band communication systems," *Int. J. Advances Engin. Technol.*, **8**, 3, 2015, p. 337.

[14] E. Agastra, G. Pelosi, S. Selleri and R. Taddei, "Taguchi's method for multi-objective optimization problems," *Int. J. RF Microw. Comput.-Aid. Eng.*, **23**, 3, 2013, pp. 357-366.

[15] G. Pelosi, S. Selleri and R. Taddei, "A novel multi-objective Taguchi's optimization technique for multi-beam array synthesis," *Microw. Opt. Technol. Lett.*, **55**, 8, 2013, pp. 1836-1840.